Ibn Al Haitham Journal for Pure and Applied Science

Journal homepage:http://jih.uobaghdad.edu.iq/index.php/j/index

Thickness Effect of CuAlTe2 Thin Films on Morphological, Structural and Visual Properties

Noor A. Hassan **Iman Hameed Khudayer**

Department of Physics, College of Education for Pure Sciences / Ibn Al-HaithamIbn University of Baghdad

Nooralhudahassam84@gmail.com

Article history: Received 1July 2019, Accepted 9October 2019, Published in July 2020.

Doi: 10.30526/33.3.2471

Abstract

$CuAlTe_2$ thin films were evaporation on glass substrates using the technique of thermal evaporation at different range of thickness (200,300,400and500) ±2nm. The structures of these films were investigated by X-ray diffraction method; showing that films possess a good crystalline in tetragonal structure. AFM showed that the grain size increased from (70.55-99.40) nm and the roughness increased from (2.08-3.65) nm by increasing the thickness from (200-500) nm. The optical properties measurements, such as absorbance, transmtance, reflectance, and optical constant as a function of wavelength showed that the direct energy gap decreased from (2.4-2.34) eV by the gain of the thickness.

Key word: Thin Film, Optical Properties, Thermal Evaporation.

1. Introduction

I-III-VI2 compound are ternary isoelectronic equivalents of the *II-VI* binary compounds. They crystallize in these chalcopyrite structure that closely for zinc blend. Completely these materials have direct band gaps [1]. Ternary ceramic is attractive materials in promising photovoltaic and optoelectronic requests [2, 3]. Like smart windows, coating films for IR reflection, transparent electrodes in plane panel show, functional glasses and solar cells [4, 5]. Single crystal has a direct forbidden band gap Eg =2.06 eV. It can be used for example in window with other ternary compounds, $CuAlTe_2$ film is found to be p-type, and some of electrical properties annealed $CuAlTe_2$ thin film at 300C, it also found that there are two X-ray diffraction peaks at 2Θ=24.60and 45.20 corresponding respectively to (112) and (220,204) orientation of the $CuAlTe_2$ chalcopyrite phase. Thin film was deposited using several methods: sputtering [6]. Elemental co-evaporation [7]. Flash evaporation [8]. And electrodeposition [9]. Thin films employed in this study were prepared from a single source technique using thermal evaporation.

2. Theoretical

Absorbance (A) is defined as the proportion between the intensity of the absorbed radiation (I_A) and of the incident radiation (I_0) [10].

$$\mathbf{A=I_A/I_0} \quad (1)$$

Transmission (T): is the ratio between transmission intensity radiation of the film (I_T) to the incident radiant intensity (I_0), otherwise reflectance (R) is the ratio between reflected radiation intensities (IR) and (I_0) as in formula [10].

$$\mathbf{R=I_R/I_0} \quad (2)$$

The reflectivity was created for all prepared films as in the equation [10].

$$A+T+R=1 \quad (3)$$

The absorption coefficients of $CuAlTe_2$ thin film depend on the values of the incident photon (hυ) and the type of optical electronic transfer. When the photon beam incident on the thin film component part of it is reflected, other transmitted and third absorbed by the film material. Absorption coefficient (α) represented the attenuation that happened in the energy of incident photon for unit thickness, which attributed to the acculturation processes.

We can deduce from the absorption or transmission spectra using the Lambert Law [11, 12].

$$I=I_0\, e^{-\alpha t} \quad (4)$$

Where, I is the total radiation, t is the film thickness.

$$\alpha t=\ln(I_0/I) \quad (5)$$

$$\alpha t=2.303\mathrm{Log}(I_0/I) \quad (6)$$

The absorption of the film (A) could be defined as [10].

$$\alpha=2.303 \quad (7)$$

To calculate the optical energy gap for direct transition used the following equation [13].

$$\alpha h\upsilon = D\,(h\upsilon - Eg)^r \quad (8)$$

r represents constant and can take values 1/2,3/2,2 and 3 depending on the type of the optical transition and the material.

Extinction coefficient is the exponential decay of the wave that passes through the medium [14].

$$k=\alpha\lambda/4\pi \quad (9)$$

The complex refractive index with real and imaginary parts as in the equation [15].

$$n_{complex}= n_0-ik \quad (10)$$

Where no could be evinced by the formula [16].

$$n_0= (4R/(1-R)^2{-}k^2)^{1/2}+ (1+R/1-R) \quad (11)$$

The R is the The reflectivity, as show below [17].

$$R= (n_o-1)^2+k^2/(n_o+1)^2+k^2 \quad (12)$$

The real (ε_r) and imaginary part (ε_i) of dielectric constant can be estimated utilizing the following equation [18-19].

$$\varepsilon_{complex}=\varepsilon_r-\varepsilon_i \quad (13)$$

$$\varepsilon_r=n_0^2-k^2 \quad (14)$$

$$\varepsilon_i=2n_ok \quad (15)$$

AFM is an imaging technique employed to evaluate the physical properties of dielectrics, conductors and semiconductor surfaces; it supplies us with very exact data about surface roughness average (r.m.s), as well as grain size [20]. It is an important tool for nanoscale, that it bears a very high-resolution amount of (0.1nm), Zoom power is estimated at (5 × 102 -108) with the power to operate under normal atmospheric pressure without the need for the high vacuum [20]. The structure of the $CuAlTe_2$ deposited films were studied by XRD method by Siemens x-ray diffractometer method, that recorded the intensity as a functions of Bragg angles [21]. From two of consecutive lattice plane, the term 2dsinθ of the diffraction of X-rays for crystalline materials are [22].

$$n\lambda_{X\text{-Ray}} = 2d\sin\theta \tag{16}$$

The lattice constant values in Tetragonal system can be computed from the following equations using the Miller incidents (hkl) and the inter-planar spacing (d) [23].

$$1/d^2 = (h^2+k^2/a^2) + l^2/c^2 \tag{17}$$

3-Result and discussion

Figure 1. Show the XRD pattern for thin $CuAlTe_2$ film that deposited on glass substrate with many thickness (200, 300,400, and 500) nm. The blueprints showed that all the films have polycrystalline mode. The first peak located at $2\theta \approx 25.96$ with the (112) preferred orientation, when the second peak appeared at $2\theta \approx 27.16$ with the (103) one. **Table 1.** showed the structural parameters, the results showed that the film had a good crystalline in tetragonal structure and the intensity increased with the increasing of the thickness [24, 25, 26] with a simple shift at the distinctive peaks. This was due to the different conditions of preparation of the

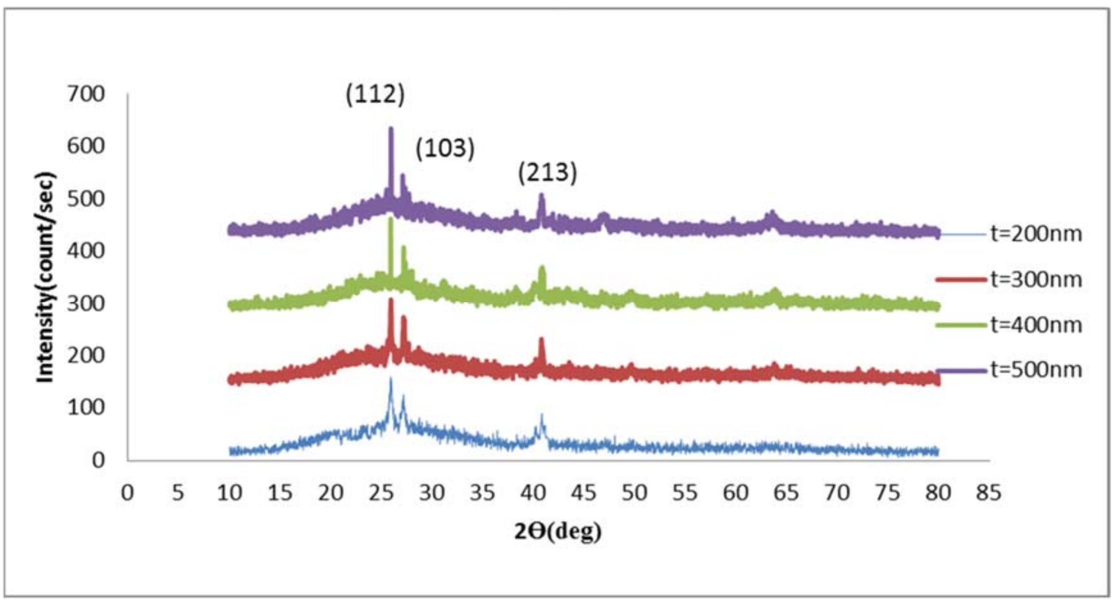

Figure 1. XRD pattern of thin $CuAlTe_2$ films with the thicknesses (200, 300, 400 and 500).

Table 1. Structural parameter of thin $CuAlTe_2$ films with the thicknesses (200, 300, 400 and 500), size crystal (64,2 66.3, 68.0 and 74.8) respectively.

Thickness (nm)	2Θ Std. (deg)	2Θ (Exp) (deg)	dhkl (Std.) (Å)	dhkl (Exp.) (Å)	hkl
200	25.96	25.9	3.42	3.40	112
	27.16	27.18	3.27	3. 23	103
	40.86	40.84	2.206	2.25	213
300	25.96	25.94	3.42	3.46	112
	27.16	27.18	3.27	3.30	103
	40.86	40.8	2.206	2.20	213
400	25.96	25.92	3.42	3.41	112
	27.16	27.2	3.27	3.24	103
	40.86	40.84	2.206	2.208	103
500	25.96	25.9	3.42	3.40	112
	27.16	27.1	3.27	3.22	103
	40.86	40.8	2.206	2.21	103
	63.08	63.06	1.47	1.45	008

In parliamentary law, to examine the surface topography, roughness of thin films and the impression of film thickness on it, we used the atomic force microscope (AFM), which possessed the ability to get very precise statistical values about the texture size and surface roughness values depending on the root mean square (r.m.s.). **Figure 2.** Represented AFM images in two and three-dimensional forms for $CuAlTe_2$ thin film with different thickness (t = 200,300,400,500) nm. The average grains size was improved as the increase of film thickness increased as presented, this was too supported by the X-ray diffraction pattern and indicated the improved structural properties of the films of high thickness by decreasing synthetics defects such as the vacancy and grainboundary, leading to an increase in the particle size of the film. The roughness of the surface was increased as; these results are listed in **Table 2.**

A

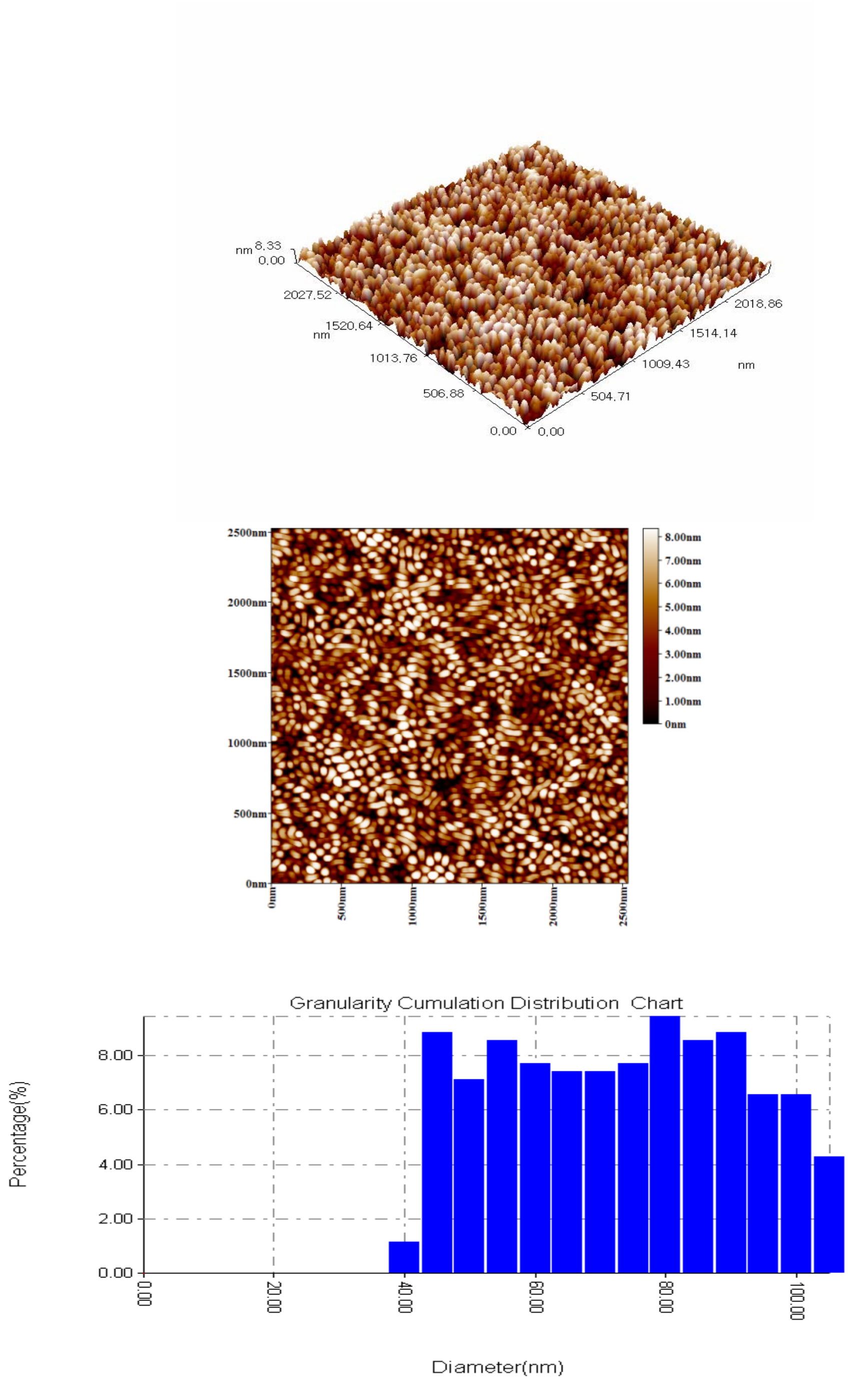
nm 8.33
0.00
2027.52
nm 1520.64
1013.76
506.88
0.00
0.00
504.71
1009.43
1514.14
2018.86
nm
2500nm
2000nm
1500nm
1000nm
500nm
0nm
0nm
500nm
1000nm
1500nm
2000nm
2500nm
8.00nm
7.00nm
6.00nm
5.00nm
4.00nm
3.00nm
2.00nm
1.00nm
0nm
Granularity Cumulation Distribution Chart
Percentage(%)
8.00
6.00
4.00
2.00
0.00
0.00
20.00
40.00
60.00
80.00
100.00
Diameter(nm)

B

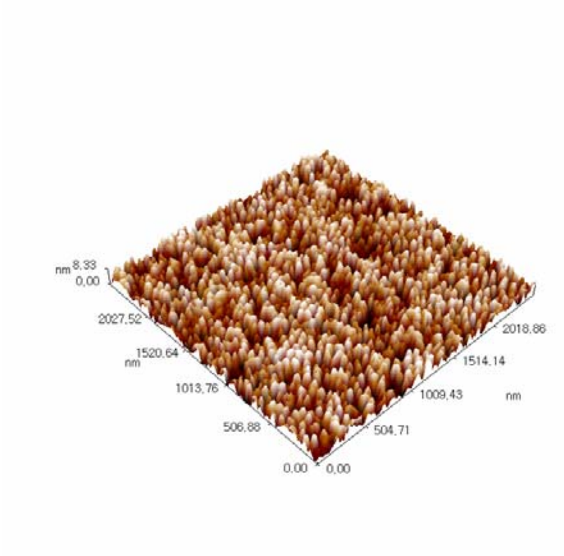
nm 8.33
0.00
2027.52
1520.64
nm
1013.76
506.88
0.00
0.00
504.71
1009.43
1514.14
2018.86
nm

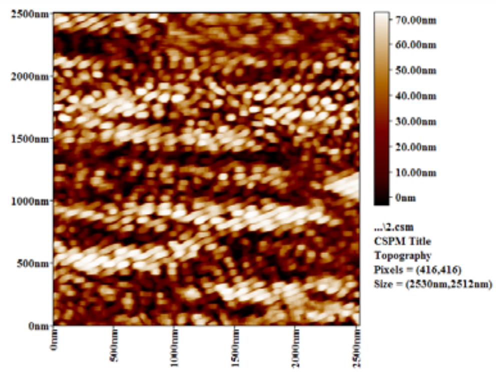
2500nm
2000nm
1500nm
1000nm
500nm
0nm
0nm
500nm
1000nm
1500nm
2000nm
2500nm
70.00nm
60.00nm
50.00nm
40.00nm
30.00nm
20.00nm
10.00nm
0nm
...\2.csm
CSPM Title
Topography
Pixels = (416,416)
Size = (2530nm,2512nm)

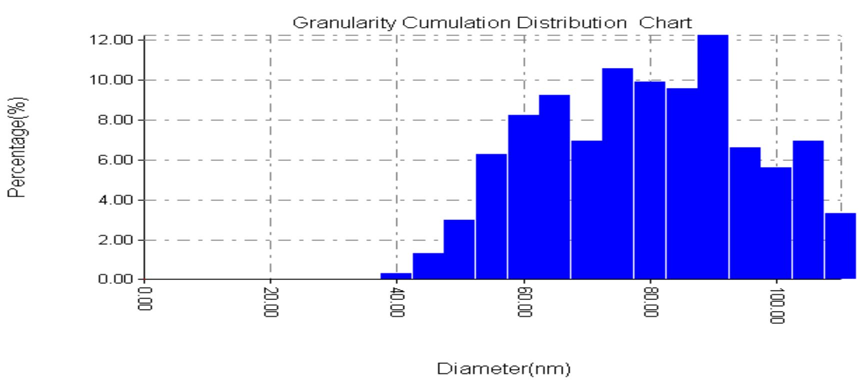
Granularity Cumulation Distribution Chart
Percentage(%)
12.00
10.00
8.00
6.00
4.00
2.00
0.00
0.00
20.00
40.00
60.00
80.00
100.00
Diameter(nm)

C

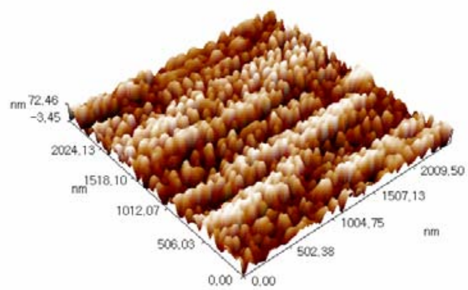
nm 72.46
-3.45
2024.13
nm 1518.10
1012.07
506.03
0.00
0.00
502.38
1004.75
1507.13
2009.50
nm

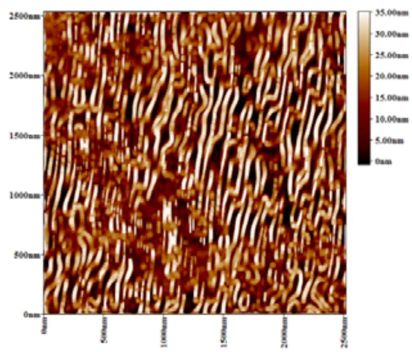

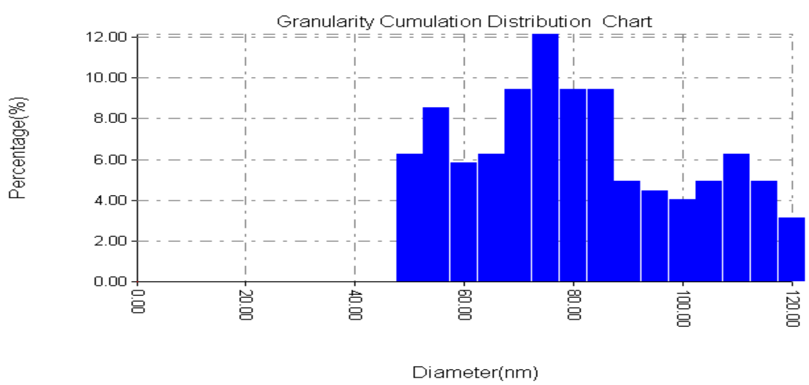
Granularity Cumulation Distribution Chart
Percentage(%)
12.00
10.00
8.00
6.00
4.00
2.00
0.00
0.00
20.00
40.00
60.00
80.00
100.00
120.00
Diameter(nm)

D

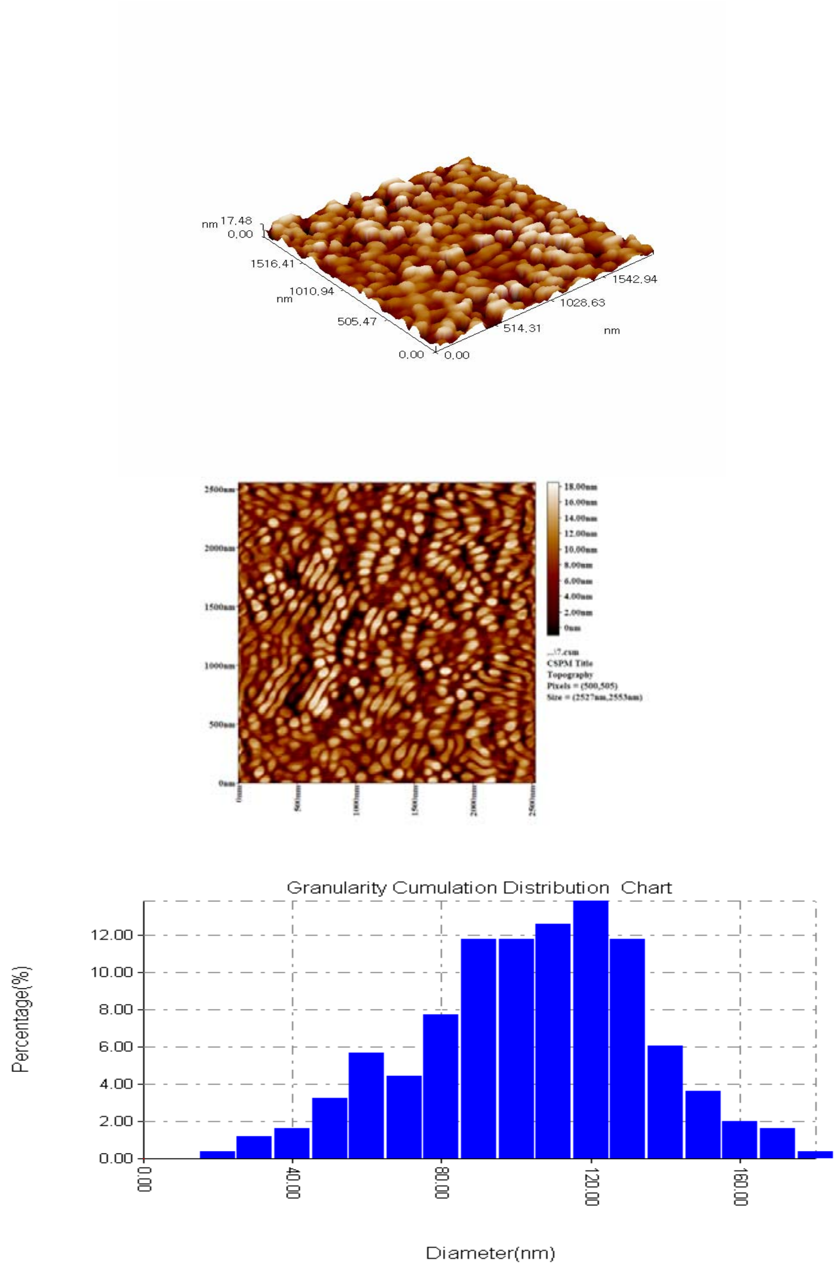

Figure 2. AFM image of thin $CuAlTe_2$ film at different thickness (A=200, B=300, C=400 and D=500) nm.

Table 2. Average grain size (G.S) and roughness average of thin $CuAlTe_2$ films with the thicknesses (200, 300, 400 and 500).

Thickness (nm)	Grain size (G.S) (nm)	Roughness average (nm)	r.m.s (nm)
200	70.55	2.08	2.4
300	76.66	18.8	21.7
400	78.34	8.98	10.4
500	99.40	3.65	4.39

The absorbance spectra for thin film with different thickness were presented in **Figure 3.** It was demonstrated that absorbance increased with the decrease of wavelength when it was closer to the visible spectrum (400-700) nm which indicated the possibility of the use of $CuAlTe_2$ films in the solar cell industry, while decreased to the lowest values at the wavelengths (near IR). Also it was observing from **Figure 3.** That absorbance increased with increasing of thickness reaching to high absorbance over (80%) in the visible region when t= 500 nm, that agreement with Murugan and Murali [27-29]. This increasing can be attributed to the improved crystalline arrangement and the decreasing of crystalline defects, the bigger crystalline sizes were formed and in this case extra atoms existing in the $CuAlTe_2$ films so extra states would be available of the photons to be absorbed [30,31]. Within the visible region (400-700) nm of the electromagnetic spectrum [32,33].The increase of the absorption in general by increasing the thickness of the film, which was due to the increase of the degree of crystallization of the film preparation - by increasing the thickness - and then the increase of the particle size of the resulting. Consequently the photon falling on the surface of the film preparation would suffer from successive absorption by the crystals within the grain and thus the possibility of reflection within the grain and thus the possibility of reflection or transmission without being absorbed by electrons. The compound atoms will be few, especially by increasing the size of the grain (ie, increasing the number of crystals in it by increasing thickness. As the number of these crystals increases, the falling photon will capability more absorption attempts than before the atoms of those crystals, which leads to the absorption of the whole and then increases the absorption factor, especially when low photonic energies, these high absorptions indicate the possibility of use these prepared films in photovoltaic solar cells or as an antireflection cover in the visible region of the electromagnetic spectrum.

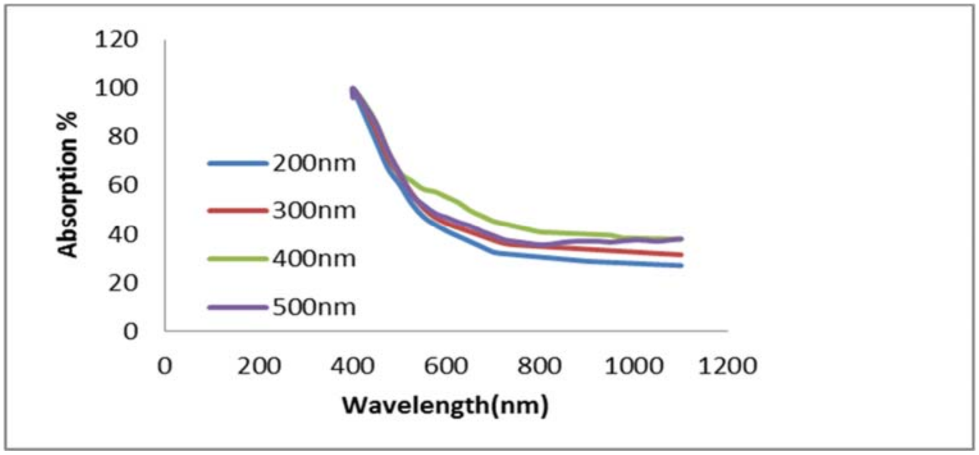

Figure 3. The absorbance spectral for CuAlTe2 films with different thickness.

Figure 4. Shows transmittance spectra for $CuAlTe_2$ thin films at many thickness. The lower transmittance in the visible region, this property represents an important and convenient in solar cell applications. On the other hand, there is a high transmission in the direction of the infrared (IR) of the electromagnetic spectrum and this indicates the possibility of using these films as a window in this region of the electromagnetic spectrum and the signals reaches it [34].

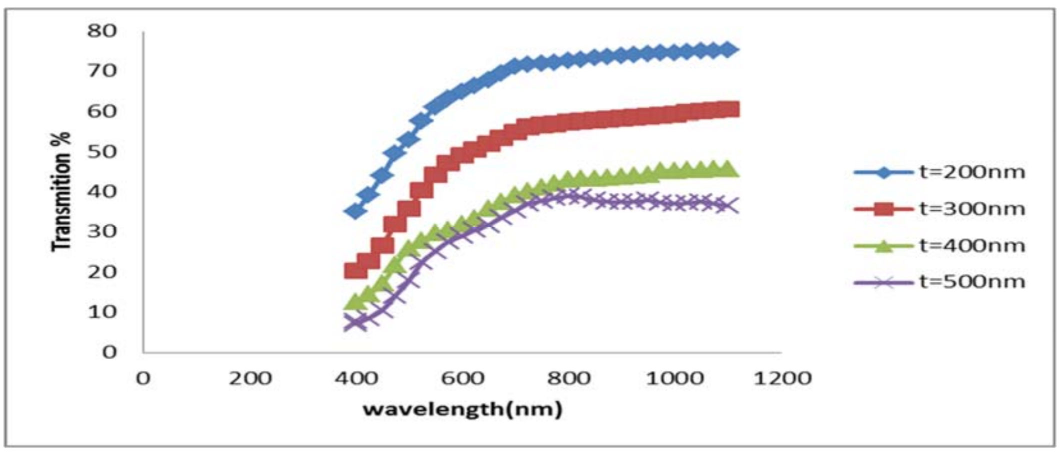

Figure 4. The transmittance spectral for $CuAlTe_2$ films with different thickness.

The reflectance of the incident spectrum shown in the **Figure 5.** And the amount of it depend on the incident wavelength, the surface roughness, and the angle between the incident beam and the surface of the cell.

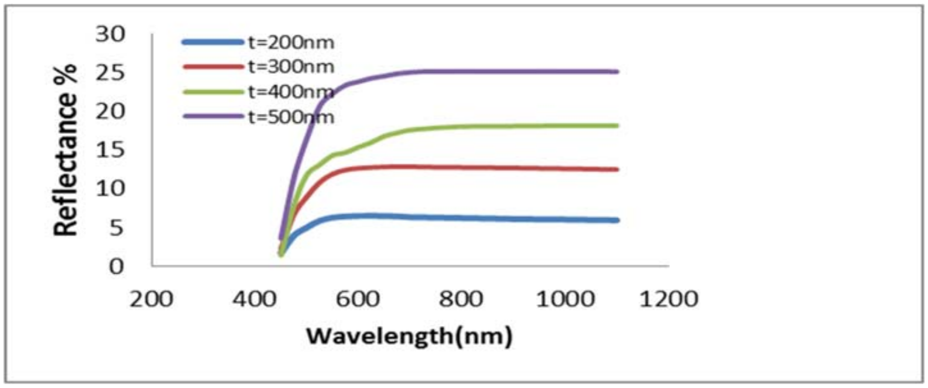

Figure 5. The reflectance spectra of $CuAlTe_2$ films at different thickness.

The absorption coefficient (α) behavior is very similar to the Absorption spectrum (A) because of the proportionally between them according to the equation (7). From the high values of absorption coefficient ($\alpha > 10^4$ cm^{-1}), it can be recorded that the band gap is direct and this is consistent with [35, 36]. We likewise note that the values of absorption coefficient (α) of the films is increasing when it is high to the visible spectrum region. The increases of absorption coefficient with the increasing of thickness as indicated in **Figure 6.** This is consistent with the effects of obtaining structural test. The cause for this is ascribable to the nature of the relationship between Absorption and absorbance factor adds to the improvement in the level of crystallization Material of the film by increasing thickness.

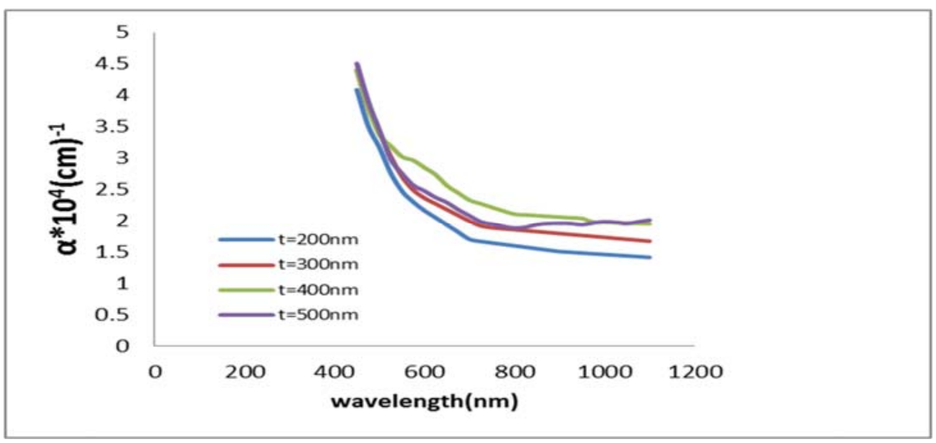

Figure 6. The Absorption Coefficient for $CuAlTe_2$ films with different thickness

The optical band gap values obtained using equation (8). The value of optical energy gap decreases with increasing of thickness for all samples as indicated in **Figure 7.**

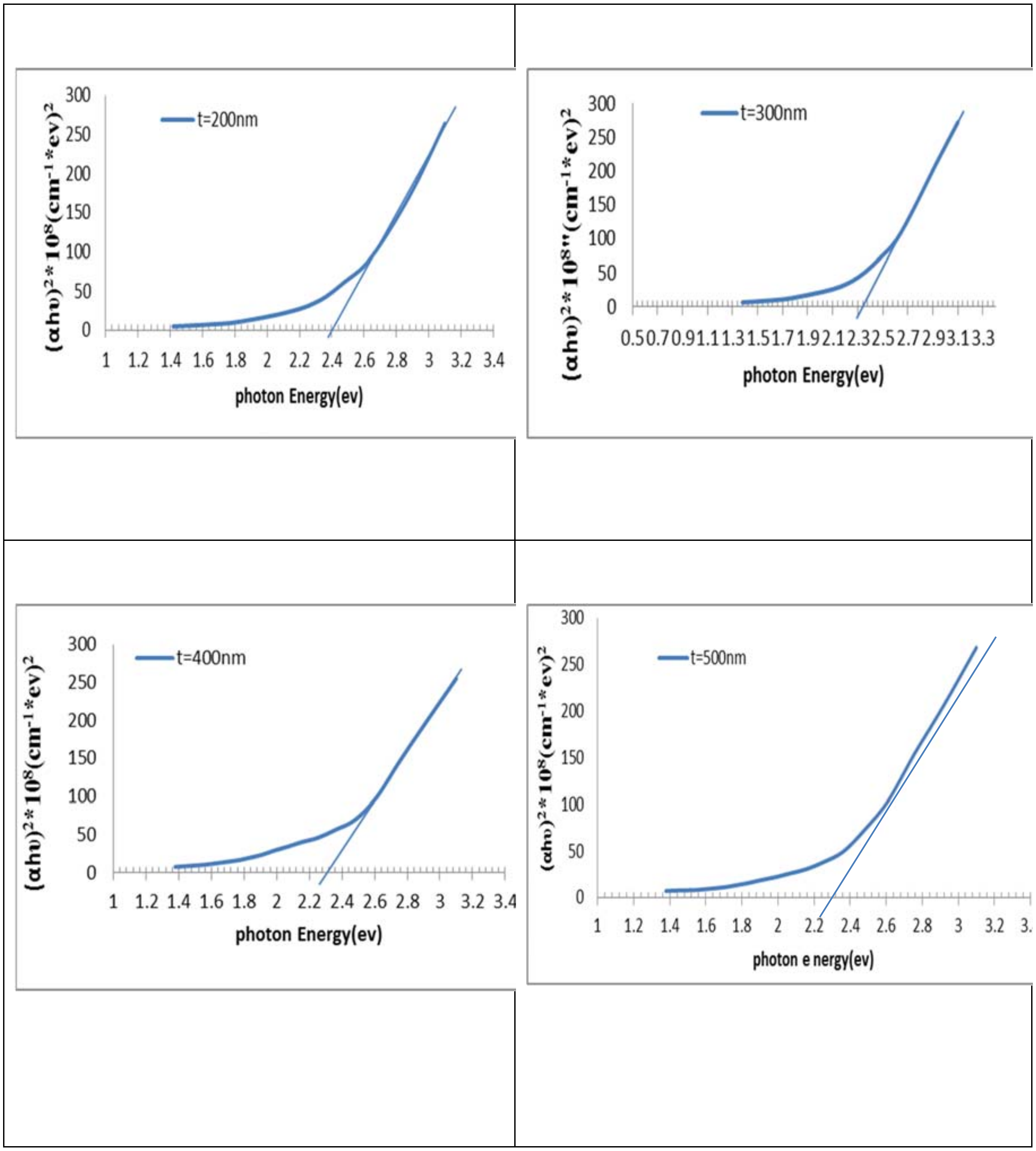

Figure 7. $(\alpha h\upsilon)^2$ vs. $h\upsilon$ for $CuAlTe_2$ films with different thickness

Table 3. Presents the decreasing of the allowed direct band gap and optical constant at wavelength (500nm) with the gain of thickness, which can be attributed to the increase of particle size [37]. One can notice the E_g^{opt} value of film with thickness 200 nm has 2.4 eV; this value is in good agreement with [38].The reason for this decrease is due to the so-called effect size Quantum, meaning that if the particle size is much larger than the diameter of Bohr and the equal to half of the Angstrom, then the quantitative effect will appear and the value of the energy gap will change in reverse proportion with the grain radius square according to the Schrödinger equation for the energy level. The consequences of the structural tests of the

atomic force microscope showed that there was a clear increase in particle size by increasing thickness - as in **Table 2.** Which led to the decrease observed in the value of the energy gap.

Table 3. Direct band gap and optical constant for $CuAlTe_2$ thin films of different thickness.

t(nm)	Eg(eV)	α*10^4 cm^{-1}	n	k	ε_r	ε_i
200	2.4	3.166625	1.570577	1.2606E-05	2.4667112	3.96E-05
300	2.35	3.416116667	1.850126	1.35992E-05	3.4229645	5.032E-05
400	2.32	3.3681375	2.039627	1.34082E-05	4.1600802	5.47E-05
500	2.34	3.445288	2.361573	1.37153E-05	5.5770267	6.478E-05

We can note from **Figure 8.** That the variation of extinction coefficient with film thickness is non- regular, this is credited to the similar reason mentioned earlier in the absorption coefficient because the behavior of extinction coefficient is similar to the absorption coefficient, and the reason for increase the absorption coefficient is the case of direct electronic transitions.

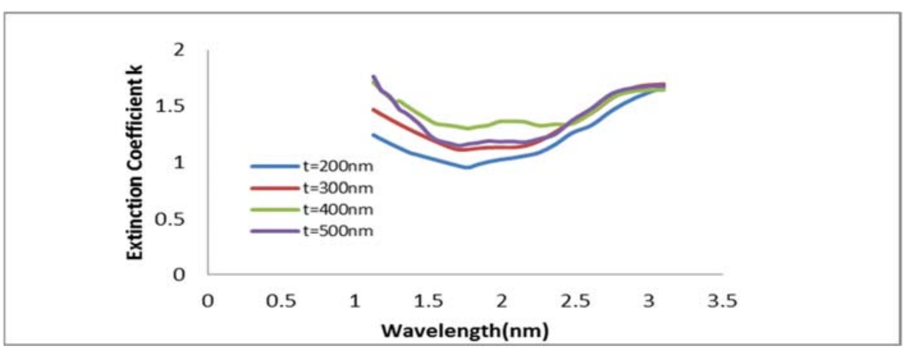

Figure 8. Extinction Coefficient for $CuAlTe_2$ films with different thickness.

The refractive index that is shown in **Figure 9.** Indicates the increase in the values with the gain of the thickness, which can explain the prepared samples denser (the increasing of the packing density), which in turn decreases propagation velocity of light through them, which resulting in the increasing of no values since not represent the ratio of light velocity through the vacuum to velocity through any medium.

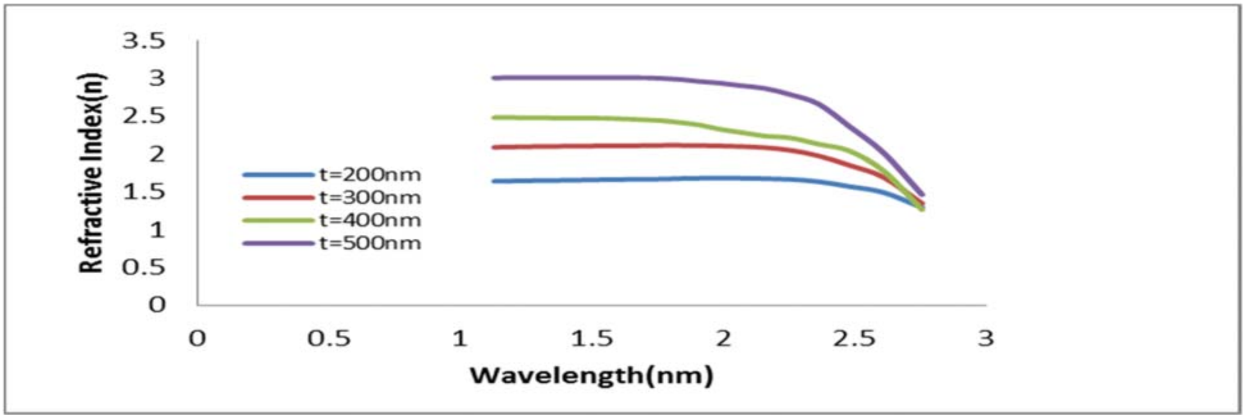

Figure 9. Refractive Index for $CuAlTe_2$ films with different thickness.

Figure 10. Shows the behavior of the real part of the dielectric constant as a subroutine of the wavelength. We note that the mode of (εr) is similar to that of the refractive index, which is due to the decreased values of k^2 compared with n^2 in (equation14).

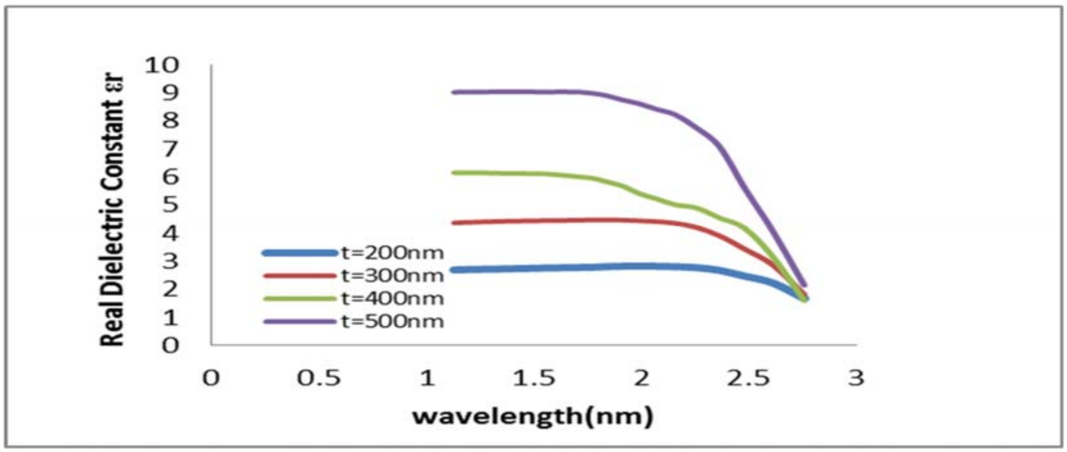

Figure 10. Real dielectric constant for $CuAlTe_2$ films with different thickness

Figure 11. Depicts the imaginary dielectric constant value as functions for wavelengths. The imaginary part of the dielectric constant is a measure of the absorption of radiation energy by free carriers of material atoms. It has a behavior similar to that of extinction coefficient, which is related to the variation of absorption coefficient also the figure determines, that increased with the increasing of thickness.

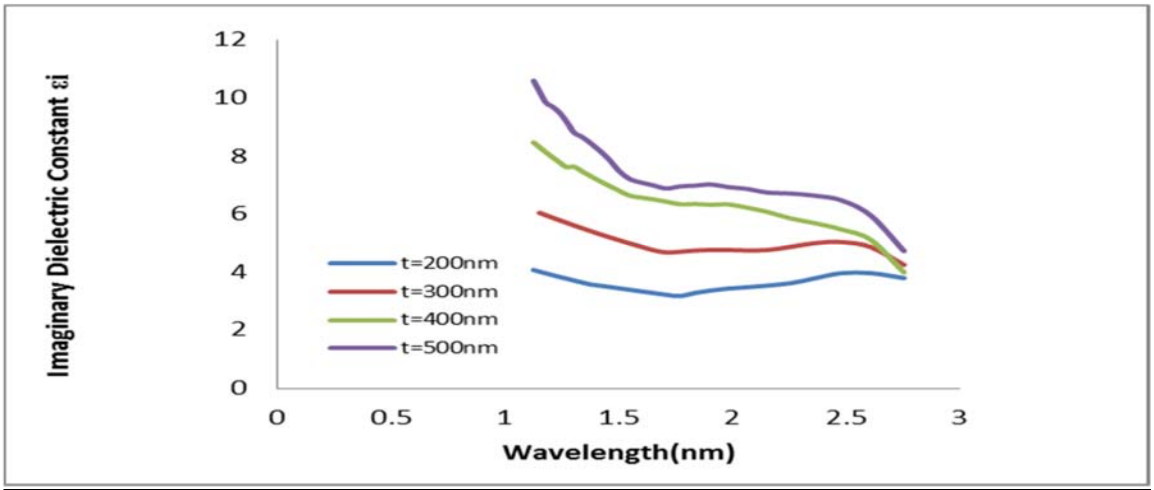

Figure 11. Imaginary dielectric constant for CuAlTe2 films with different thickness.

4. Conclusion

Thin films [39]. Have polycrystalline with Tetragonal unit structures with preferential orientation in the (112) direction. Grain size and roughness increased with the increasing of thickness. It was noted that all prepared thin films have high absorption, in the visible range of the electromagnetic spectrum, which made it desirable for the fabrication of solar cells, the optical transitions in $CuAlTe_2$ were direct optical energy gap, and it decreased from (2.34-2.4) eV with the increasing of thickness from (200-500) nm.

References

1. Korzun, B.V.; Fadzeyeva, A.A.; Bente, K.; Schmitz, W.; Schorr, S. Thermal expansion and structural properties of (CuAlTe2)1-x (CuAlSe2) x solid solutions, Cryst. Res. Technol*Journal of Experimental and Industrial Crystallography*.**2006**, *41*, *2*, 168 – 173.
2. Bente, K. Structural Aspects of Ternary Compounds-Crystal Structure, Chemical Bonding, Substitution, Defects and Semiconductivity of Multinary Compounds. Japanese *Journal of Applied Physics*.**2000**, *39*, *S1*, 1.
3. Rau, U.; Schock, H.W. Electronic properties of Cu (In, Ga) Se2 heterojunction solar cells–recent achievements, current understanding, and future challenges. *Applied Physics A*.**1999**, *69*, *2*, 131-147.
4. Guha, S.; Yang, J.; Banerjee, A.; Glatfelter, T.; VenduraJr, G.J.; Garcia, A.; Kruer, M. July. Amorphous silicon alloy solar cells for space applications. In *Proc. of the 2nd World Conference and Exhibition on Photovoltaic Solar Energy Conversion*, **1998**.
5. Pfisterer, F. The wet-topotaxial process of junction formation and surface treatments of Cu2S–CdS thin-film solar cells. *Thin Solid Films*.**2003**, *431*, 470-476.
6. Horinaka, H.; Yamamoto, N. Japanese Research Review for Pioneering. Ternary and Multinary Compounds in the 21st Century *IPAP*.**2001**, 348.
7. Picozzi, S.; Zhao, Y.J.; Freeman, A.J.; Delley, B. Mn-doped CuGaS 2 chalcopyrites: An ab initio study of ferromagnetic semiconductors. *Physical Review B*.**2002**, *66*, *20*, 205206.
8. Larsen, E.M. Zirconium and hafnium chemistry. In *Advances in Inorganic Chemistry and Radiochemistry*.**1970**, *13*, 1-133.

9. Chahboun, N.; Assali, K. El Khiara, A.; Ameziane, E.L.; Bekkay, T. Sol. Energy Mater. Sol. Cells.**1994**, *32*, 213.
10. Ome, M.A. Elementary Solid State Physics, Addiso-We sly Publishing, **1975**.
11. Kavasoglu, A.S.; Bayhan, H. Admittance and impedance spectroscopy on Cu (In,Ga)Se2 Solar cells, *Turkish Journal of Physics*.**2003**, *27*, 529-535.
12. Sen, Zekai. *Solar energy fundamentals and modeling techniques: atmosphere, environment, climate change and renewable energy*. Springer Science & Business Media, **2008**.
13. RutuparnaMohanty, *Electronic Properties of Ternary and Binary Compounds*, Thesis Submitted for the Award of the Degree of Master of Science, Department of Physics National Institute of Technology,**2012**.
14. chopra, K.LA. Thin film Phenomena, Mc.Grew-hill Book compan, Chapter one 3 rd edition, **1987**.
15. Rabhi, A.; Kanzari, M. Effect of air annealing on CuSbS2 thin film grown by vacuum thermal evaporation. *Chalcogenide Letters*.**2011**, *8*, *4*, 255-262.
16. Buba, A.D.A.; Adelabu, J.S.A. Optical and Electrical Properties of Chemically Deposited ZnO Thin Films, the Pacific *Journal of Science and Technology*.**2010**, *11*, 2, 429-434.
17. Rajesh, K.R.; Menon, C.S. Electrical and Optical Properties of vacuum Deposited ZnPc and CoPc Thin Films and application of variable range hopping model, Indian *journal of pure & applied physics*.**2005**, 43.
18. Kittle, C. Introduction to Solid State Physics, John Wiley and Sons Inc., 8th edition. **2005**, 964-971.
19. Rodriguez-Carjaval, J. FullProfRietveld, Profile Matching & Integrated Intensities, Refinement of X-ray and/or Neutron Data, version 2.0 *LLB, Saclay, France*, **2001**.
20. Tribble, A. Electrical Engineering Materials and Devices, University of Lowa, **2002**.
21. Colakoglu, T. The Effects of Post-Annealing Process on The Physical Properties of Silver-Indium-Selenium Ternary Semiconductor Thin Films Deposited by Electron Beam Technique, Ph.D. Thesis in Physics Department of Middle East Technical University, **2009**.
22. William Callister, D. *Materials Science and Engineering:An Introduction*, 7th Edition, John Wiley & Sons, USA, **2007**.
23. Cullity, B.D. elements of X-Ray diffraction, 2 nd edition, copyright © by Addison – Wesley Publishing company, Inc, **1978**.
24. Mishra, S.; Ganguli, B. Effect of p-d hybridization and structural distortion on the electronic properties of AgAlM2 (M = S,Se,Te) chalcopyrite semiconductors,*Solid state communications*.**2011**, *151*, 7,1-15.
25. Moreh, A.U.; Momoh, M.; Yahya, H.N.; Isah, K.U.; Hamza1, B. The Effect of Thickness on Structural Properties of CuAlS2 Thin Films by Thermal Evaporation, *Journal of Physical Science and Innovation*.**2013**, *5*, *2*, 111-119.
26. Chih-Hao Lee, Fong-Gang Guo, and Chia-Chin Chu, The Thickness Dependent of Optical Properties, Resistance, Strain and Morphology of Mo Thin Films for The Back Contact of CIGS Solar Cells, *Chinese Journal Of Physics*.**2012**, *50*, *2*.
27. Eaton, P.; West, P. Atomic Force Microscopy, Oxford University Press Inc, *New York*, **2010**.

28. Miller, P.; Yang, R. Scanning Tunneling and atomic force microscopy combined, *Applied Physics Letters*.**1988**, *52*, 2233-2235.
29. Murugana, S.; Muralib, K.R. Structural Optical and Electrical Studies on Pulse Plated AgInSe2 Films, *Acta Physics Polonica* A.**2014**, *3*, *126*, 727-731.
30. Deng, B.; Wei, Q. WeidongGao. Physical properties of Al-doped ZnO films deposited on nonwoven substrates by radio frequence magnetron sputtering, *Journal of Coating Technology and Research*.**2008**, *5*, *3*, 393- 397.
31. Sheua, J. K.; Lee, M.L. Ultraviolet band-pass Schottky barrier photodetectors formed by Al-doped ZnO contacts to n-GaN, *Applied physics letters*.**2006**, *88*, 043506.
32. Pankove, J. Optical Processes in Semiconductors, Prentice – Hall, Inc., Englewoodcliffs *New Jersey*.**1971**, *285*,111.
33. Weiner, R. ed. Nanoelectronics and Information Technology: *Advanced Electronic Materials and Novel Devices*. Wiley-VCH, **2005**.
34. Prabahar, S. Balasubramanian, V.; Suryanarayanan, N.; Muthukumarasamy, N. Optical properties of copper indium diselenide thin films, Chalcogenide Letters *Baghdad Science Journal*.**2010**, 49–58.
35. Ahmad, S.; Mohib-ulHaq, M. A study of energy gap, refractive index and electronic polarizability of ternary chalcopyrite semiconductors, *Iranian Journal of Physics Research*.**2014**, *14*, *3*, 89-93.
36. ParthaDey, Joe Bible, SomnathDatta, Scott Broderick, JacekJasinski, MahendraSunkara, MadhuMenon and Krishna Rajan, Informatics-aided bandgap engineering for solar materials, *Computational Materials Science*.**2014**, *83*, 185–195.